RSC Advances




ROYAL SOCIETY OF CHEMISTRY

www.rsc.org/advances

RSC Advances

ARTICLE

# Photodeposition synthesis of ZnO nanoporous layer

Received 00th January 20xx,
Accepted 00th January 20xx

DOI: 10.1039/x0xx00000x

www.rsc.org/advances

Jia-Jian Guan[a], Hao-Qi Wang[a], Hong Liang[b], Nan-Pu Cheng[a], Hua Lin[a], Qing Li[a], Yuan Li[a] and Li-Zhao Qin[a]*

An original photodeposition methodology is investigated to synthesize novel ZnO nanoporous layer with high uniformity and pore density via $TiO_2$ nanotube substrate(annealed at 450℃ under $10^{-2}$Pa for 8 hours) immersed in $Zn(NO_3)_2$ aqueous solution(1mol.$L^{-1}$) and irradiated by ultraviolet(UV) light at room temperature for 12 hours. Material characterization highlights that nanoporous layer is assembled by dominant $(10\bar{1}1)$ crystal plane of hexagonal wurtzite ZnO, with vertical sheet thickness about 20nm and aperture diameter around 100nm. Vacuum annealing of $TiO_2$ substrate ultimately impacts the uniformity of ZnO nanoporous layer, which can be essentially attributed to the density of substrate oxygen vacancies. The concentration of $Zn(NO_3)_2$ aqueous solution, however, significantly influences the morphology and pore density of porous layer. Furthermore, ZnO nanoporous layer enhances the photoelectric property of pure $TiO_2$ nanotubes, which may provide general application prospects in photocatalysis and photoelectric devices.

## Introduction

Synthesis of functional materials with controllable morphologies and orientations has attracted sustained attention in material science and technology, since material and device performances are extremely sensitive to surface structures at the nanoscale. The synthetic processes, however, remain significant challenges such as homogeneous nucleation and aligned growth on material surface; nevertheless, basic principles of photochemical processes on semiconductor surface stimulate an original inspiration for us to synthesize functional materials with desired structures and performances.

Zinc oxide(ZnO), one of the most competitive functional materials, exhibits extensive application prospects in semiconductor devices[1-8]owing to its wide band gap, large exciton binding energy, and extraordinary thermal, electrical, optoelectronic properties[9]. In particular, ZnO nanostructures with various morphologies and dimensions such as nanodots, nanowires, nanobelts, and nanoflowers[10-14] have broadly been investigated. Among which, nanoporous ZnO emerges excellent performances in gas sensor, photocatalysis, and solar cell applications[15-17]due to high surface-to-volume ratio and efficient transport capability. However,a photodeposition method to synthesize high-quality ZnO nanoporous layer has not been reported yet.

Typical technologies to fabricate ZnO nanostructures attribute to wet-chemical method, because the morphology and structure can be effectively controlled by altering the synthesis conditions at a relatively low temperature compared with the approaches of magnetron sputtering[18,19], chemical vapor deposition(CVD)[20-22], vapor phase transport deposition[23], and thermal evaporation[24,25]. By wet-chemical strategy, ZnO nanostructures are normally synthesized via zinc ions($Zn^{2+}$) reacting with hydroxide ions($OH^-$) under an appropriate solution concentration, system pressure, and reaction temperature. Conventionally, zinc nitrate($Zn(NO_3)_2$), zinc chloride($ZnCl_2$), and zinc acetate($Zn(CH_3COO)_2$) serve as the source of $Zn^{2+}$; sodium hydroxide(NaOH) and potassium hydroxide(KOH) are mainly used to provide $OH^-$. Especially, $Zn(NO_3)_2$ solution act as both $Zn^{2+}$ and $OH^-$ sources, followed by ZnO self-assembly processes on templates with the help of organic molecule $C_6H_{12}N_4$[26]. However, a strong reaction process occurs to the mixture aqueous solution of $Zn^{2+}$ and $OH^-$, which is unfavorable to control compared with a moderate method. In terms of organic solvents, although they contribute to facilitating ZnO assembling process, simultaneously, organic molecules and impurities are brought in products, which can not completely eliminate.

Unlike wet-chemical method, electrochemical approach can interfere reaction process by providing external electrons in solution, which significantly increase the opportunity to assemble

[a] Faculty of Materials and Energy, Southwest University, Chongqing 400715, People's Republic of China. E-mail: qin8394@163.com; Tel: +86-023-68253204
[b] Key Laboratory of Beam Technology and Material Modification of Ministry of Education, Beijing 100875, People's Republic of China.

chemical substances on substrates. G.R.Li et al[27] used $ZnCl_2$ solution to fabricate self-assembled ZnO nanoporous structures on Cu substrates by electrochemical deposition at 90℃, however, organic reagent was used to control the shape of nanoporous structures. Z.F.Liu et al[28] used $Zn(NO_3)_2$ solution and template assistant to obtain porous ZnO films by electrochemical deposition at 70℃, which is inconvenient for template preparation. In contrast to electrochemical method, a photodeposition approach seems like more practical, economy and environment-friendly without using sophisticated equipment, templates or organic additives. Our research group has fabricated ZnO/$TiO_2$ hierarchical structures on pure Ti sheets via a soft photodeposition approach[29] of anneal 1h+$Zn(NO_3)_2$ 0.01M+UV 1h, however, a low yield and disorganized distribution of as-prepared ZnO nanostructures essentially limit its application. In this work, we investigate the formation process of ZnO molecules further and redesign the synthesis condition. In consequence, a novel ZnO nanoporous layer with high yield and uniformity emerges under the synthesis condition of anneal 8h + $Zn(NO_3)_2$ 1M + UV 12h.

## Experimental

In experiments, titanium dioxide($TiO_2$) nanotubes were prepared as reaction substrate for the following reasons: (i) $TiO_2$ acts as photoelectron source due to its sensitive UV excitation response; (ii) $TiO_2$ nanotubes exhibit large surface area and high defect density, which are beneficial to molecule absorption and ZnO nucleation. As depicted in Fig.1, pure titanium(Ti,99.9%) sheets(2cm × 1cm × 0.5mm) were firstly dipped in nitric acid ($HNO_3$, 67.5ml, 65.0~68.0wt%) and hydrofluoric acid(HF, 15ml, 40.0wt%) mixture aqueous solution with stirring for 30 seconds, then ultrasonically cleaned in acetone and deionized water, respectively. Secondly, using the etched titanium sheet as anode and platinum(Pt) sheet as cathode to electrolyze hydrofluoric acid aqueous solution(HF, 100ml, 1.0wt%) under 20V direct current(DC) power for 20 minutes, then ultrasonically cleaned in deionized water. Thirdly, annealing(1h and 8h, respectively) the as-oxidized titanium sheets under $10^{-2}$ Pa at 450℃. The as-annealed titanium sheets were finally immersed in zinc nitrate hexahydrate($Zn(NO_3)_2 \cdot 6H_2O$) aqueous solution(1mol·$L^{-1}$ and 2mol·$L^{-1}$, respectively) at room temperature, followed by sustained UV irradiation(1h and 12h, respectively; 1000W high pressure Hg lamp, the strongest emission wavelength is 365nm); the distance between titanium sheets and liquid surface particularly requires less than 1mm to restrain the decay of photon density on titanium surface, then ultrasonically cleaned in deionized water and dried at 50℃ for 1 hour.

The morphologies of products were observed by field emission scanning electron microscopy(FESEM, Hitachi S4800) at an accelerating voltage of 10kV. The structures were analyzed by transmission electron microscopy(TEM, JEM-2100) at an accelerating voltage of 200kV, X-ray diffraction(XRD, Shimadzu XRD7000) with Cu Kα( λ =1.5418Å) incident radiation at a scanning rate of 4° per minute, and Raman spectroscopy(Horiba Jobin Yvon, LavRAM Aramis) with laser wavelength at 532nm.

The performance of photocurrent response versus time(I-t) was investigated by electrochemical workstation CHI-604C under intermittent illumination in a 2-electrode system. ZnO/$TiO_2$ photoelectrode(sample d) and $TiO_2$ photoelectrode were respectively used as one electrode(working electrode), Pt sheet was used as the other electrode(counter+reference electrode); $Na_2SO_4$ aqueous solution(0.01mol·$L^{-1}$) was used as electrolyte; high pressure Hg lamp(500W, the strongest emission wavelength is 365nm) was used as the light source.

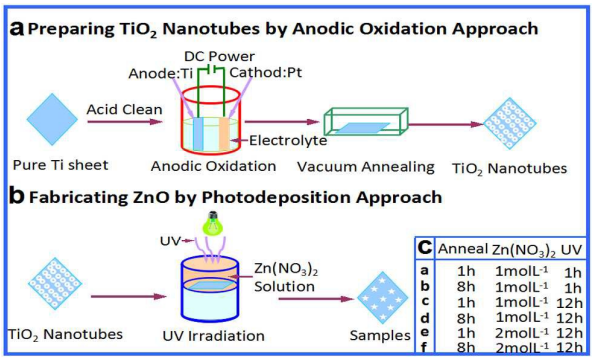


**Fig.1.** Process illustration of preparing ZnO/$TiO_2$ hierarchical structures (a) anodic oxidation approach to prepare $TiO_2$ nanotube substrate,(b) photodeposition approach to fabricate ZnO nanoporous layer on substrate, (c) detailed synthesis parameters of sample a to sample f.

## Results and discussion

FESEM images presented in Fig.2 show intuitive observation of as-prepared samples under distinct synthesis conditions. Sample a(Fig.2a) and sample b(Fig.2b), with substrate immersed in $Zn(NO_3)_2$ aqueous solution(1mol·$L^{-1}$) and irradiated by UV light for 1 hour, reflect initial nucleation; notably, vacuum annealing for 8 hours(Fig.2b) yields bulk nuclei on substrate with high uniformity. Along with an increased time(12 hours) of UV irradiation, porous configurations that constructed by vertical sheets have emerged in sample c(Fig.2c) and sample d(Fig.2d); similarly, vacuum annealing for 8 hours(Fig.2d) enhances the uniformity and pore density of porous structures with aperture diameter about 100nm. Especially, with an extended time(12 hours) of UV irradiation and an increased concentration(2mol·$L^{-1}$) of $Zn(NO_3)_2$ aqueous solution, the sheets become thin and disorganized as shown in sample e(Fig.2e) and sample f(Fig.2f).

The XRD pattern as depicted in Fig.3a reveals crystal structure of sample d(Fig.2d). In contrast to the $TiO_2$ nanotubes, sample d exhibits strong peak at 35.3°(2θ) that index to (10$\bar{1}$1) plane of hexagonal wurtzite ZnO(JCPDS No.75-1533); the peak at 25.2°(2θ) belongs to (101) plane of anatase $TiO_2$(JCPDS No.21-1272). Fig.3b shows detailed molecular structure of sample d analyzed by Raman

spectra. The peaks at 437.2cm$^{-1}$ and 610.7cm$^{-1}$ attribute to the inherent non-polar $E_2$(high) phonon mode and $E_1$(LO) phonon mode of hexagonal wurtzite ZnO, respectively. The peaks at 150.7($E_g$), 201.2($E_g$), 395.4($B_{1g}$), 513.5($B_{2g}$), and 633.0($E_g$) cm$^{-1}$ index to anatase $TiO_2$. Further information about the nanoporous structures of sample d can be obtained from the high resolution TEM(HRTEM) image in Fig.2g. The interplanar spacing is about 0.25nm, which is parallel to the (10$\bar{1}$1) plane spacing of wurtzite ZnO.

In brief, ZnO nanoporous layer is obtained with $TiO_2$ substrate(8h vacuum annealing) immersed in $Zn(NO_3)_2$ aqueous solution(1mol·L$^{-1}$) and irradiated by UV light for 12 hours. Noticeably, vacuum annealing of substrate influences the initial ZnO nucleation, which ultimately determines the uniformity of porous structures. Time of UV irradiation, however, plays an indispensable role on crystal growth; with dominant sheet growth of ZnO (10$\bar{1}$1) plane and favorable concentration of $Zn(NO_3)_2$ aqueous solution(1mol·L$^{-1}$), porous configuration was finally assembled on (101) surface of anatase $TiO_2$.

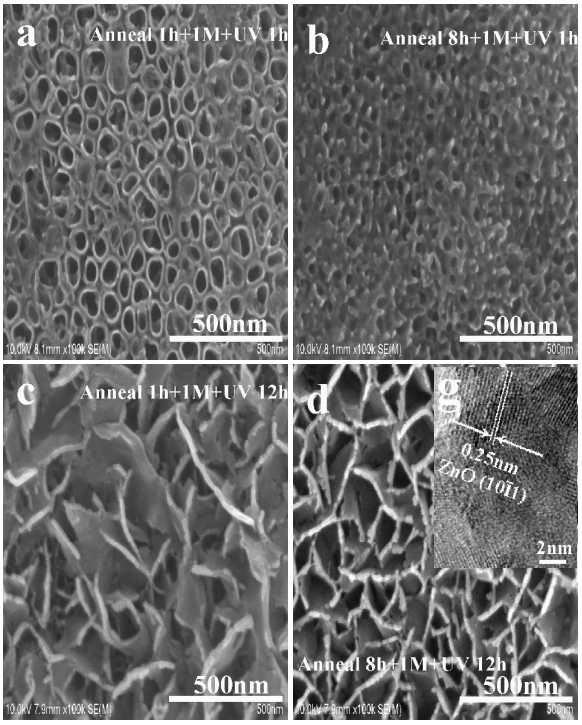


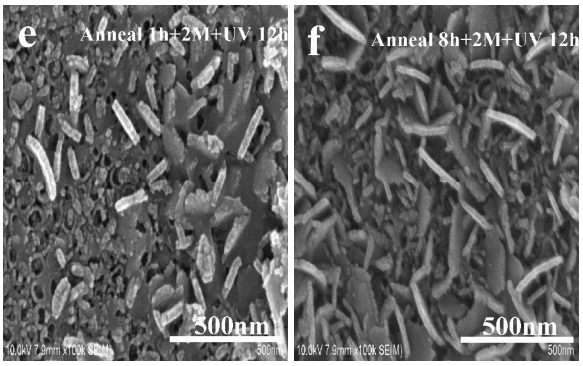


**Fig.2.** FESEM and High resolution TEM(HRTEM) images of as-prepared ZnO nanoporous layer with distinct synthesis conditions(Fig.1c): (a) FESEM image of sample a, (b) FESEM image of sample b; (c) FESEM image of sample c, (d) FESEM image of sample d, (e) FESEM image of sample e, (f) FESEM image of sample f, (g) HRTEM image of surface layer structure corresponding to sample d.

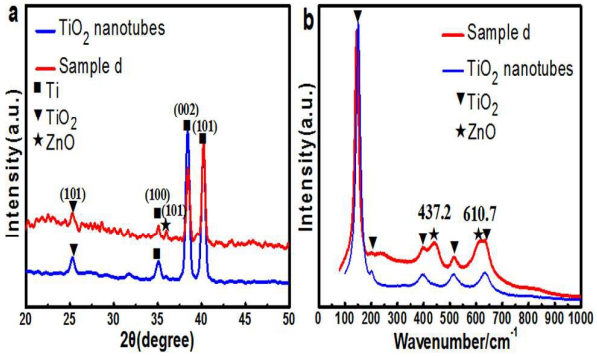


**Fig.3**. (a) XRD pattern of as-prepared sample d and $TiO_2$ nanotubes, (b) Raman spectra of as-prepared sample d and $TiO_2$ nanotubes.

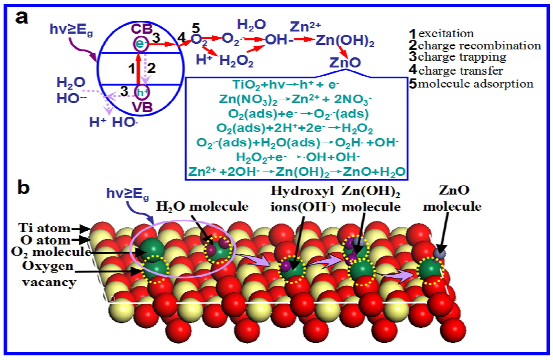


**Fig.4.** Theoretical formation processes of ZnO molecules synthesized by photoelectrochemical approach. (a) typical reaction equations with UV irradiating $Zn(NO_3)_2$ aqueous solution; (b) The reaction processes on the (101) surface of anatase $TiO_2$ with UV irradiating $Zn(NO_3)_2$ aqueous solution.

Fig.4 shows theoretical formation process of ZnO molecules corresponding to the experiments of figure 2. Photogenerated electrons are stimulated from valance band to conduction band of

$TiO_2$ under the UV irradiation. Surface and bulk trapping firstly occur to these conduction band electrons within picoseconds to nanoseconds[31], and partial trapped electrons can be transferred to interface of $TiO_2$ nanotubes within microseconds to milliseconds[32] ignoring the recombination of surface trapping. Then, oxygen molecules in $Zn(NO_3)_2$ aqueous solution will capture interfacial electrons and become superoxide radical anions ($O_2^{\cdot-}$)[33]. The superoxide radical anions typically react with absorbed water molecules to form hydroperoxyl radicals($O_2H^{\cdot}$) and hydroxyl ions($OH^-$); Simultaneously, oxygen molecules and hydrogen ions($H^+$) can absorb interfacial electrons to obtain hydrogen peroxides($H_2O_2$). The hydrogen peroxides accept excess electrons to form hydroxyl radicals($^{\cdot}OH$) and hydroxyl ions. Ultimately, hydroxyl ions react with Zinc ions($Zn^{2+}$) to generate unstable Zinc hydroxid($Zn(OH)_2$) that will decompose into Zinc oxide(ZnO) and coat on the surface of $TiO_2$ nanotubes.

According to the above theory, the nucleation and growth of ZnO crystal structures on $TiO_2$ surface should essentially determined by the following factors: (i) the density of surface electrons; (ii) the distribution of absorbed oxygen molecules; (iii) the concentration of Zinc ions. As for the process of crystal nucleation, the emergence of oxygen vacancies affect the electron density and molecule absorption for the following reasons: (i)oxygen vacancies provide localized $Ti^{3+}$ states, which act as trap centers for photogenerated charge carriers(holes and electrons)[34] and help to absorb surface molecules; (ii)oxygen vacancies increase the electron density of conduction band, which behave as an n-type semiconductor[35,36]. Bulk oxygen vacancies emerge in the crystal lattices by vacuum annealing, therefore, substrate annealing treatment plays an indispensable factor that influence the nucleation of ZnO nanoporous structures. The following process of crystal growth is partially depended on the equilibrium of water molecule and Zinc ions, which can be effectively coordinated by providing $Zn(NO_3)_2$ aqueous solution with a suitable concentration of $1mol{\cdot}L^{-1}$. The time of UV irradiation, however, should be long enough(12h) till the crystal growth entirely accomplished.

In order to investigate the photoelectric property of ZnO nanoporous layer(sample d), typical photocurrent-time response curves was measured in a 2-electrode system as shown in Fig.4. After 250 seconds(5 cycles), both sample d and $TiO_2$ nanotubes exhibit stable tendency of photocurrent response performance under intermittent illumination, and the transient photocurrent density of sample d nearly rises to 0.15 $mA{\cdot}cm^{-2}$, which is 3 times stronger than $TiO_2$ nanotubes with 0.05 $mA{\cdot}cm^{-2}$. In conclusion, the I-t curves obviously illustrate that ZnO nanoporous structures greatly enhance the photoelectric property of $TiO_2$ nanotubes, and this result can be explained for the following reasons: the nanoporous act as transport paths for solution molecules and increase the reaction opportunities; On the other hand, the charge carrier recombination can be alleviated by coupling another semiconductor owing to the physical separation[30], which is equivalent to increasing the photocurrent density of hierarchical structures

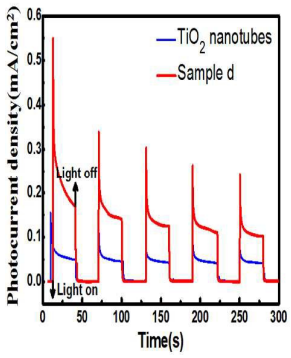


**Fig.5.** The transient photocurrent densities of ZnO/$TiO_2$ and $TiO_2$ photoelectrodes

## Conclusions

This work investigate a moderate photodeposition approach to synthesize ZnO nanoporous layer, with $TiO_2$ substrate(vacuum annealed at at 450℃ for 8hours) immersed in $Zn(NO_3)_2$ aqueous solution($1mol{\cdot}L^{-1}$) and irradiated by UV light at room temperature for 12 hours. Raman spectra, XRD pattern, and TEM image reveal that the novel porous nanostructures attribute to hexagonal wurtzite ZnO, with dominant crystal growth surface on $(10\bar{1}1)$ plane. Substrate vacuum annealing for 8 hours ultimately enhance the uniformity of ZnO nanostructures, which can be essentially attributed to the density of substrate oxygen vacancies. The concentration of $Zn(NO_3)_2$ aqueous solution significantly influence the morphology of porous layer; with a suitable concentration of $1mol{\cdot}L^{-1}$, the pore density of porous layer has been improved. The as-prepared ZnO porous structures greatly enhance the photoelectric property of $TiO_2$ nanotubes, which may have practical application prospects in photocatalysis and photoelectric devices.

## Acknowledgements

This work is partially supported by the Key Laboratory of Beam Technology and Material Modification of Ministry of Education in Beijing Normal University (No.201411), the Doctoral Foundation of Southwest University (No.104230-20710909) as well as the National Natural Science Foundation of China (No.51171156).

## References

1 N. Golego, S. A. Studenikin and M. Cocivera, *J. Electrochem. Soc.,* 2000, **147**, 1592.
2 S. Liang, H. Sheng, Y. Liu, Z. Hio, Y. Lu and H. Shen, *J. Cryst. Growth*, 2001, **225**, 110.
3 K. Keis, E. Magnusson, H. Lindstrom, S. E. Lindquist and A. Hagfeldt, *Sol. Energy*, 2002, **73**, 51.
4 R. L. Hoffman ,B. J. Norris and J. F. Wager, *Appl. Phys. Lett*., 2003, **82**, 733.
5 D. C. Look, B. Claflin, Y. I. Alivov and S. J. Park, *Phys. Stat. Sol.,* 2004, **201**, 2203.
6 Q. Wan, Q. H. Li, Y. J. Chen, T. H. Wang, X. L. He, J. P. Li and C. L. Lin, *Appl. Phys.Lett*., 2004, **84**, 3654.

7 Z. L. Wang and J. H. Song, *Science*, 2006, **312**, 243.
8 M. L. Zhang, F. Jin, M. L. Zheng, J. Liu, Z. S. Zhao and X. M. Duan, *RSC Adv*., 2014, **4**, 10462.
9 Ü. ÖzgÜr, Y. I. Alivov, C. Liu, A. Teke, M. A. Reshchikov, S. Doğan, V. Avrutin, S.-J. Cho and H.Morkoç, *J. Appl. Phys*., 2005, **98**, 041301.
10 C. Pacholski, A. Kornowski and H. Weller, *Angew. Chem. Int. Ed*., 2002, **41**, 1188.
11 L. E. Greene, M. Law ,D. H. Tan, M. Montano, J. Goldberger, G. Somorjai and P. D. Yang, *Nano Lett*., 2005, **5**, 1231.
12 J. Hong, J. Choi, S. S. Jang, J. Gu, Y. Chang, G. Wortman, R. L. Snyder and Z. L. Wang, *Nano Lett*., 2012, **12**, 576.
13 B. X. Li and Y. F. Wang, *J. Phys. Chem. C*, 2010, **114**, 890.
14 R. X. Shi, P. Yang, X. B. Dong, Q. Ma and A. Y. Zhang, *Appl. Surf. Sci*., 2013, **264**, 162.
15 J. Zhang, S. Wang, M. J. Xu, Y. Wang, B. L. Zhu, S. M. Zhang, W. P. Huang and S. H. Wu, *Cryst. Growth Des*., 2009, **9**, 3532.
16 B. Pal and M. Sharon, *Mater. Chem. Phys*., 2002, **76**, 82.
17 B. Kiliç, E. GÜr and S. TÜzemen, *J. Nanomater*., 2012, DOI:10.1155/2012/474656
18 P. F. Carcia, R. S. Mclean, M. H. Reilly and G. Nunes Jr., *Appl. Phys. Lett*., 2003, **82**, 1117.
19 S. H. Jeong, B. S. Kim and B. T. Lee, *Appl. Phys. Lett*., 2003, **82**, 2625.
20 J. J. Wu and S. C. Liu, *Adv. Mater.,* 2002, **14**, 215.
21 P. C. Chang, Z. Y. Fan, D. W. Wang, W. Y. Tseng, W. -A. Chiou, J. Hong and J. G. Lu, *Chem. Mater.*, 2004, **16**, 5133.
22 J. H. Park and J. G. Park, *Current Appl. Phys*., 2006, **6**, 1020.
23 B. Daragh, F. A. Rabie, B. Teresa, G. R. David, T. Brendan, O. H. Martin and M. Enda, *Cryst.Growth Des*., 2011, **11**, 5378.
24 Z. W. Pan, Z. R. Dai and Z. L. Wang, *Science*, 2001, **291**, 1947.
25 B. D. Yao, Y. F. Chan and N. Wang, *Appl. Phys. Lett*., 2002, **81**, 757.
26 L. Vayssieres, *Adv. Mater*., 2003, **15**, 464.
27 G. R. Li, C. R. Dawa, Q. Bu, X. H. Lu, Z. H. Ke, H. E. Hong, F. L. Zheng, C. Z. Yao, G. K. Liu and Y. X. Tong, *J. Phys. Chem. C,* 2007, **111**, 1919.
28 Z. F. Liu, Z. G. Jin, W. Li, X. X. Liu, J. J. Qiu and W. B. Wu, *Mater. Lett.,* 2006, **60**, 810.
29 P. Li, H. X. Lu, L. Z. Qin, H. Liang, M. Ning and Y. Li, *Chinese J. Inorg. Chem*., 2012, **28**, 1855.
30 H. J. Zhang, G. H. Chen and D. W. Bahnemann, *J. Mater. Chem.,* 2009, **19**, 5089.
31 M. R. Hoffmann, S. T. Martin, W. Y. Choi and D. W. Bahnemann, *Chem. Rev*., 1995, **95**, 69.
32 M. A. Henderson, *Surf. Sci. Rep.,* 2011, **66**, 185.
33 K. Nakata and A. Fujishima, *J. Photochem. Photobiol. C:Photochem. Rev.,* 2012, **13**, 169.
34 A. L. Linsebigler, G. Lu and J. T. Yates Jr., *Chem. Rev.,* 1995, **95**, 735.
35 E. WahlstrÖm, E. K. Vestergaard, R. Schaub, A. RØnnau, M. Vestergaard, E. Lægsgaard, I. Stensgaard and F. Besenbacher, *Science*, 2004, **303**, 511.
36 N. S. P.-Vélez, O. O.-Neria, I. H.-Pérez and A. R.-Ponce, *Surf. Sci.,* 2013, **616**, 115.